Dielectric Characterization of a Thermotropic Liquid Crystalline Copolyesteramide: 1. Relaxation Peak Assignment

A. Boersma, J. van Turnhout,* and M. Wübbenhorst

Department of Polymer Technology, Faculty of Applied Science, Delft University of Technology, Julianalaan 136, 2628 BL Delft, The Netherlands

Received November 3, 1997; Revised Manuscript Received July 13, 1998

ABSTRACT: Dielectric relaxation analysis was carried out on the main chain thermotropic liquid crystalline copolyesteramide Vectra B950. The dielectric spectra of Vectra B950 show four relaxations, instead of three as cited in the literature. These correspond, from high to low temperature, to the glass transition, the rotation of hydroxynaphthoic acid moieties, the rotation of terephthalic acid moieties, and the combined rotation of terephthalic acid and aminophenol moieties. The combination of TSD and DMA analysis made it possible to distinguish between dipole and charge relaxations. Although the TSD and the dielectric results compare well for the low-temperature dipole relaxations, they are not directly comparable for the α relaxation. TSD experiments reveal that free charges have a significant influence on the α relaxation.

I. Introduction

Dielectric Spectroscopy on Liquid Crystalline Polymers. Dielectric spectroscopy on liquid crystalline polymers has attracted increasing interest in recent years to investigate the molecular motions of the main chain segments. Most of the research was focused on hydroxybenzoic acid−hydroxynaphthoic acid polymers (HBA−HNA). For these polymers, Blundell et al.[1] and Alhaj-Mohammed et al.[2] attributed the three relaxations they observed, i.e., the α relaxation to the glass transition, the β relaxation to the HNA residue, and the γ relaxation, to the HBA residue. Much attention was also paid to the dynamic mechanical properties of these polymers (Kalika et al.,[3] Troughton et al.,[4] Wissbrun et al.,[5] and Sarlin et al.[6]). Similar research has been done on LCPs derived from HBA (Green et al.,[7] Takase et al.,[8] Bechtoldt et al.,[9] and Kalika et al.[10,11]).

Although much work has been devoted to the HBA−HNA polymers, very little attention has been paid to the HNA−terephthalic acid−aminophenol copolyesteramide under study in this paper (Vectra B950). Some dynamic mechanical experiments have been performed by Wissbrun et al.,[5] Gonzalez et al.,[12] and Abdul Jawad.[13] The only dielectric experiments on the copolyesteramide were done by Abdul Jawad et al.[14] They all found a strong α and β relaxation, but no γ relaxation. We will show that this was caused by the limited frequency range used. We have obtained more detailed information about all relaxation processes present, by increasing the frequency range and by using a new method of data analysis.

TSD Spectroscopy on Liquid Crystalline Polymers. The thermally stimulated discharge/current technique (TSD/TSC) has been rediscovered for research on liquid crystalline polymers in the last years. Its high sensitivity for dipole rotations is one of the advantages of TSD. In particular, the characterization of molecular motions around the glass transition benefits from the use of this technique. Sauer et al.[15,16] have recently published two papers in which they describe the use of TSD in combination with DSC for studying the glass transition in liquid crystalline polyesters. They concluded that the glass transition observed with TSD is very broad; the temperature range ΔT of the transition is broader ($\Delta T \approx 160$ °C) than could be determined by DSC. The broad glass transition in the liquid crystalline random copolyesters is attributed to structural heterogeneities of the chains.

The TSD response of the liquid crystalline copolyester (Vectra A900) has been examined by Collins et al.,[17] Ibar,[18] and Shimizu et al.[19] Collins et al. used the thermal sampling method to investigate the activation energy as a function of poling temperature. This thermal sampling technique (also known as thermal peak cleaning or thermal windowing) makes it possible to zoom in on specific parts of the α relaxation peak. It involves polarization in a small temperature window. The dipoles that are able to rotate within this temperature window are lined up and frozen in. A depolarization peak is obtained after reheating the partially poled sample. Each depolarization thermogram can be converted to an Arrhenius plot of the relaxation time vs the inverse temperature. A lot of polymers show so-called compensation behavior, which means that after extrapolation, all lines in the Arrhenius plots converge to one point: the compensation point. This was also found by Collins et al.[17] for Vectra A900. Moura Ramos et al.[20] claim that the difference between this compensation point and the glass transition temperature is related to the width of the glass transition. Shimizu et al. claim to have found a sub-T_g relaxation, which appeared at certain poling temperatures. However, this relaxation was not found by other authors.

Scope of This Paper. In this paper, we focus on the dielectric characterization of the liquid crystalline thermotropic copolyesteramide Vectra B950. We have performed several dielectric and thermally stimulated discharge experiments in order to study the relaxation behavior in detail. The use of a 2-dimensional fitting technique made it possible to separate the various secondary relaxations and attribute them to the different motions of the main chain segments. A combination of TSD and dynamic mechanical analysis (DMA) is introduced in order to separate dipole relaxations from charge relaxations.

10.1021/ma9716138 CCC: $15.00
Published on Web 09/25/1998

II. Theory

Modeling of the Dielectric Experiments. The dielectric experiments carried out in this paper yield the complex permittivity as a function of temperature and frequency. This complex permittivity can be written as:

$$\epsilon^* = \epsilon' - i\epsilon'' \tag{1}$$

where ϵ' is the real part of the permittivity and ϵ'' is the imaginary part or dielectric loss. Various empirical equations have been derived to describe the frequency dependence of the permittivity. One of the most general is the Havriliak−Negami (HN) equation

$$\epsilon^* = \epsilon_\infty + \frac{\Delta\epsilon}{(1 + (i\omega\tau)^{\alpha_{HN}})^{\beta_{HN}}} \tag{2}$$

in which ϵ_∞ is the permittivity at optical frequency ($\epsilon_\infty = n^2$), $\Delta\epsilon$ the relaxation strength, and ω the angular frequency and α_{HN} and β_{HN} are the shape parameters of the relaxation function. All relaxations presented in this paper were fitted using this equation. The temperature dependence of the relaxations is accounted for by assuming a temperature-dependent relaxation time, $\tau(T)$. This relaxation time can depend on the temperature in two ways. The first is the well-known Arrhenius equation, which holds for thermally activated secondary relaxations:

$$\tau = \tau_\infty e^{E_A/RT} \tag{3}$$

Here, τ_∞ is the preexponential factor, which for local motions is of the order of 10^{-13} s, E_A the thermal activation energy of the dipole rotation (kJ/mol), and R the gas constant (8.314 J/mol/K).

However, when the rotations of the dipoles are determined by the free volume in the polymer, which is the case for the α relaxation, the relaxation time is given by the Vogel−Fulcher−Tammann (VFT) equation:

$$\tau = \tau_\infty e^{E_V/R(T-T_V)} \tag{4}$$

Here E_V is the VFT activation energy and T_V the VFT-temperature.

Modeling of the TSD Experiments. The TSD measurements on the polymer samples result in graphs of the depolarization current vs the temperature. Van Turnhout[21,22] has carried out extensive research on the TSD of electrets, and he derived a number of equations for the evaluation of TSD results. Clearly, the dipole relaxations which cause the TSD current are governed by the same relaxation times as found in the dielectric results, because we are dealing with the same polar groups. It is therefore possible to compare the TSD data to dielectric data performed at the right frequency. Van Turnhout obtained a relation for calculating the equivalent frequency of a TSD experiment. This frequency depends linearly on the heating rate of the samples. The maximum in the current vs temperature curve can, for symmetrical relaxation processes for which the shape factor β_{HN} in eq 2 is equal to one, be calculated from

$$\frac{d}{h\,dT}\tau(T) = -1 \tag{5}$$

in which h is the inverse heating rate during the TSD experiment (with units of s/K). For secondary relaxations the Arrhenius equation, eq 3, can be used to describe the relaxation time. In case of symmetrical relaxations, the current maximum occurs at $\omega_m\tau = 1$. This results in the following expression for the angular frequency at which the TSD current shows a maximum, ω_m:

$$\omega_m = \frac{E_A}{RT_m^2 h} \tag{6}$$

Here T_m is the temperature at which the maximum in the current is reached (K). If we are dealing with the α relaxation, we have to use the VFT equation, eq 4, for the relaxation time and the angular frequency for the current maximum becomes

$$\omega_m = \frac{E_V}{R(T_m - T_V)^2 h} \tag{7}$$

The values for the activation energies and VFT temperature can be derived from the dielectric measurements.

As stated earlier, the equivalent angular frequencies at the current maximum hold for symmetrical relaxations. In most polymers the relaxations are usually not symmetrical. In that case the shape factor β_{HN} of the Havriliak−Negami relation is not equal to one. The condition (5) and $\omega_m\tau = 1$ must then be modified. For a general HN-relaxation the maximum in the loss, ϵ''_{max}, will occur at $\omega_m\tau = a(\alpha_{HN}, \beta_{HN})$, while the maximum in the current (j_{max}) will be found at $d\tau(T)/(h\,dT) = -b(\alpha_{HN}, \beta_{HN})$, whereby a and $b \geq 1$. Havriliak et al.[23] gave an implicit relation solvable for $\omega_m\tau$ at ϵ''_{max} but, unfortunately, their relation[23] is incorrect. The correct explicit equation for $\omega_m\tau$ reads

$$\omega_m\tau = \left(\frac{\sin\left[\frac{1}{2}\pi\alpha_{HN}/(1+\beta_{HN})\right]}{\sin\left[\frac{1}{2}\pi\alpha_{HN}\beta_{HN}/(1+\beta_{HN})\right]} \right)^{1/\alpha_{HN}} \tag{8}$$

It turns out that as a good approximation we can take: $a(\alpha_{HN}, \beta_{HN}) \simeq b(\alpha_{HN}, \beta_{HN})$. This implies that eq 6 holds for all types of thermally activated relaxations, both symmetrical or asymmetrical. Similarly, eq 7 is generally obeyed for VFT-type relaxations.

Furthermore, the maximum in the current from the TSD experiments can be compared to the maximum of the dielectric loss, as was shown by Van Turnhout:[22]

$$\epsilon_0\epsilon_m''E \simeq 1.47\,\frac{I_m}{\omega_m} \tag{9}$$

I_m is the maximum TSD current density (A/m^2), ϵ_m'' the maximum dielectric loss, and E the electric poling field (V/m). Clearly, the equation which must be used for the angular frequency again depends on the kind of relaxation: Arrhenius for secondary relaxations and VFT for the α-relaxation.

III. Experiments

Materials and Sample Preparation. The polymer used was a random liquid crystalline copolyesteramide composed of three monomer units, viz. 60% 2,6-hydroxynaphthoic acid (HNA), 20% *p*-aminophenol (AP), and 20% terephthalic acid (TA) (see Figure 6). This polymer is commercially available from Hoechst-Celanese as Vectra B950. The polymer was dried for 4 h at 180 °C in a nitrogen atmosphere to remove

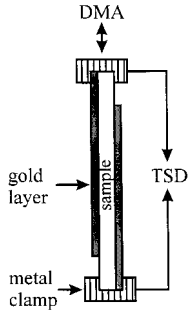

Figure 1. Setup of the combined TSD−DMA experiments. The metal clamps are isolated using the DMA 7 quartz extension measuring system and connected to the electrometer.

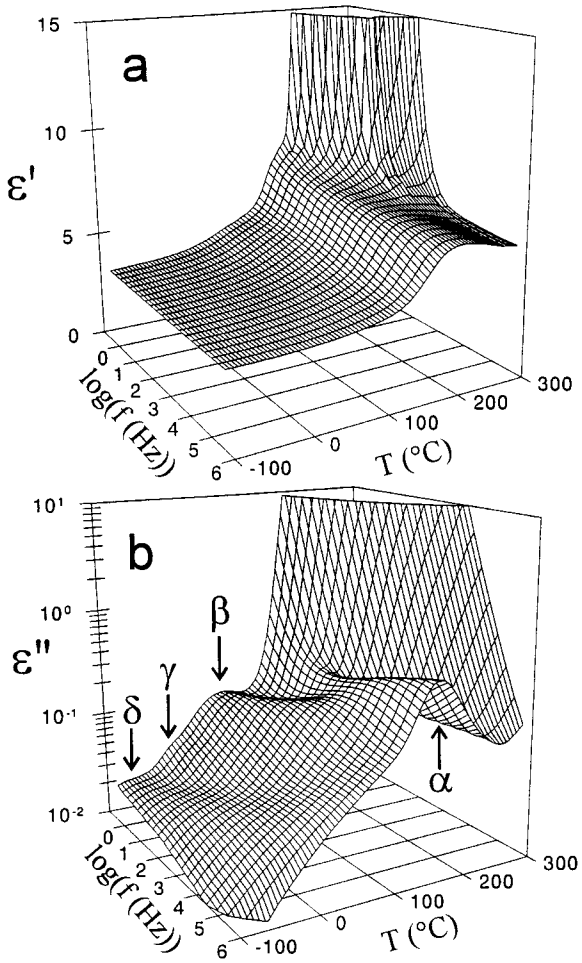

Figure 2. Dielectric permittivity (a) and loss (b) vs frequency and temperature of an extruded sample of Vectra B950 (sample E15).

residual water and kept under vacuum at 60 °C. From the dry polymer two kinds of samples were prepared.

Samples for the dielectric and TSD analysis were made by compression moulding of polymer granules at 300 °C and quenching the films afterward. The thickness of the samples was approximately 100 μm (C samples).

A second type of sample was made by film extrusion using a Collin laboratory extruder (diameter = 20 mm, length/diameter = 20). The films were drawn at the extrusion temperature (300 °C) until a certain draw ratio was reached. The resulting films varied in thickness between 10 and 200 μm. Films with various draw ratios could be prepared in this way (E samples).

DSC Experiments. The glass transition and melting temperatures of the samples were determined using a Perkin-Elmer Differential Scanning Calorimeter (DSC 7).

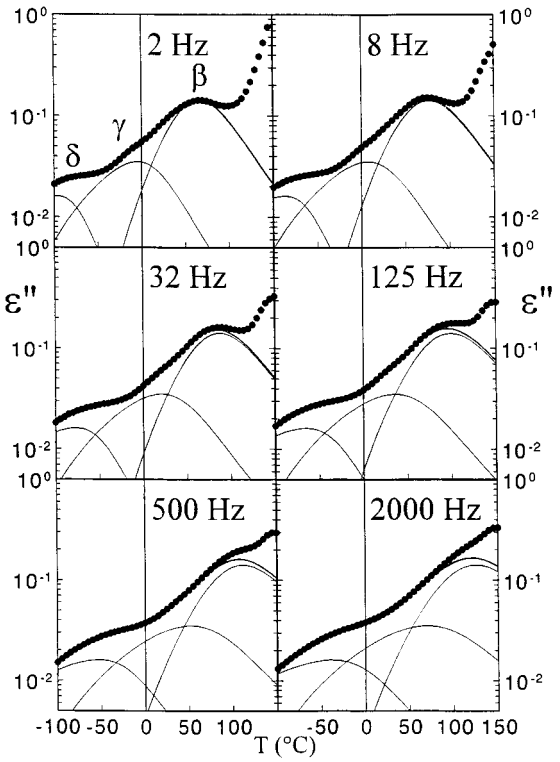

Figure 3. Dielectric loss of an extruded sample (E15) vs temperature for six frequencies (●). The part below 100 °C is fitted using three Havriliak−Negami functions for the δ, γ, and β peaks. The six frequencies are all fitted simultaneously (2D fit) which results in frequency- and temperature-independent fit parameters.

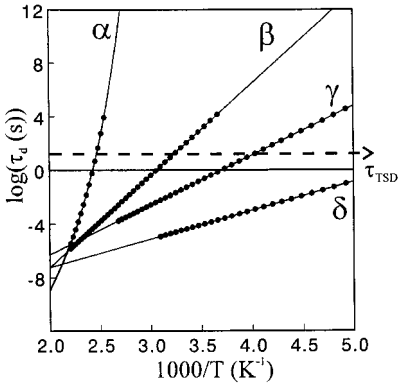

Figure 4. Arrhenius plots of the four relaxations present in Vectra B950. The dots indicate the temperature range in which the fit parameters are obtained. The equivalent relaxation time of the TSD experiments is also indicated.

Dielectric and TSD Measurements. The dielectric and TSD measurements were performed on two-sided gold sputtered films (3 cm in diameter). The sputtered samples were put between two thick brass electrodes inside a sample holder. This sample holder was then placed inside a Novocontrol temperature control unit, which regulated the temperature by means of a heated nitrogen gas flow. A Pt100 (a temperature-dependent resistor) implemented in one of the electrodes measured the temperature and ensured an as small as possible temperature gradient.

For dielectric experiments, a Hewlett-Packard 4284A precision LCR-meter was used for frequencies between 1 and 500 kHz and a combination of a Schlumberger SI 1260 impedance gain-phase analyzer and a dielectric electrometer (developed by TNO) for frequencies between 0.5 and 1000 Hz. The TSD measurements were carried out with a Keithley 487 voltage source and a Keithley 617 electrometer.

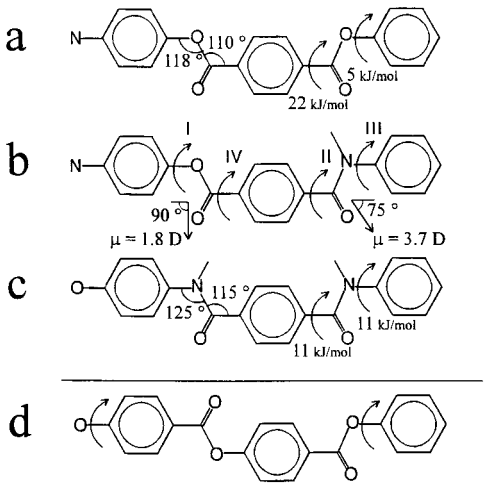

Figure 5. Possible moieties involved in the γ and δ relaxation. The bond-angle, rotation energies and dipole moments were taken from Hummel et al.[25] Rotation of a terephthalic acid group with two ester bonds (a), with one ester and one amide bond (b) and with two amide bonds (c) was observed. Joint rotation of two hydroxybenzoic acid groups in Vectra A900 was observed (d).

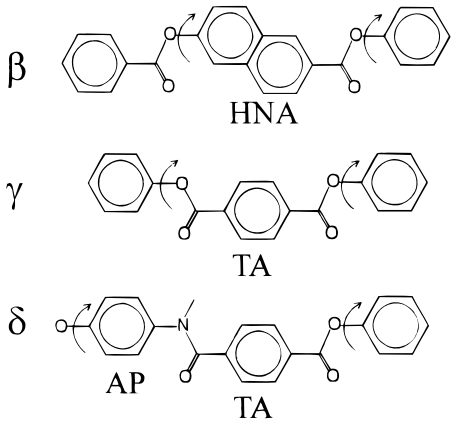

Figure 6. Assignment of the β, γ, and δ relaxation to the rotations of the three main chain moieties: HNA, TA, and AP−TA.

Dielectric measurements were done at constant temperature by taking frequency scans (0.5 Hz to 500 kHz) every 5 °C between −100 and 300 °C. The upper temperature was just above the melting point of the polymer (which is 283 °C, determined from DSC measurements at 10 °C/min). The applied AC voltage was 1 V.

During the TSD analysis, the sample was heated to a temperature T_p. At that temperature an electric DC field of approximately 1 V/μm was applied. The sample was kept at T_p for 30 min. Next, it was cooled at the rate of 4 °C/min to a temperature well below the glass transition temperature (131 °C from DSC measurements at 10 °C/min). At that point, the voltage was turned off and the sample was kept isothermally for 15 min. The depolarization current was recorded by heating the sample to 260 °C at a rate of 2 °C/min.

Combined TSD and DMA Measurements. A comparison between TSD and mechanical experiments in extension was made using a combination of a Perkin-Elmer dynamic mechanical analyzer (DMA 7e) and a Keithley 617 electrometer. To isolate the metal clamps from the rest of the setup, the DMA 7 quartz extension measuring system was used. The way the samples were sputtered is depicted in Figure 1. This made it possible to perform TSD and DMA measurements simultaneously, which was necessary in order to properly assign the peaks observed in the TSD measurements. The DMA experiments were performed using a frequency of 1 Hz.

Table 1. Fit Parameters for the α, β, γ, and δ Relaxation in Vectra B950 for Extruded Samples E15 and P15 (Values of $\omega_m\tau$ and ϵ''_{Max} Used for the TSD Calculations)

	α[a]	β	γ	δ
$\Delta\epsilon$	2.07 ± 0.15	1.11 ± 0.04	0.34 ± 0.04	0.26 ± 0.04
$\log(\tau_\infty$ (s))	−20.9 ± 0.3	−21.0 ± 0.2	−13.7 ± 0.6	−11.5 ± 0.5
E_a (kJ/mol)	46.9 ± 1.1	131 ± 5	70.8 ± 3.9	40.7 ± 2.5
T_V (K)	294 ± 2	−	−	−
α_{HN}	0.37 ± 0.09	0.40 ± 0.02	0.50 ± 0.07	0.59 ± 0.08
β_{HN}	0.43 ± 0.09	0.70 ± 0.05	0.23 ± 0.05	0.09 ± 0.04
$\omega_m\tau$	9.2	2.4	17	48
ϵ''_{max}	0.220	0.159	0.035	0.016

[a] For the α relaxation the activation energy, E_a, must be replaced by E_V.

IV. Results and Discussion

Dielectric Experiments. Assignment of the α and β Relaxation. We started our experiments by performing dielectric measurements on an extruded sample having a draw ratio of 15 (sample E15). The dielectric permittivity and loss are shown in Figure 2. The spectra of the dielectric loss vs the temperature and frequency clearly show two relaxation processes. The peak at the high-temperature side of the spectrum is the α relaxation, according to Abdul Jawad et al.[14] They ascribe this relaxation to the cooperative rotation of main chain segments and so it is related to the glass transition temperature. Interestingly, this relaxation is more pronounced than the α relaxation in similar LCPs such as Vectra A900, because of the appearance of hydrogen bonds formed by the amide and ester groups, which are only broken at elevated temperatures.

A second relaxation (β) at lower temperatures can be attributed to the rotation of the HNA units. The position of this relaxation is comparable to the peak position of the same group in Vectra A900. The relaxation parameters for the α and β relaxations were derived by fitting the frequency scans at each temperature to a Havriliak−Negami function. The shape factors of the H−N function (α_{HN} and β_{HN}) appear to be more or less constant over a very broad temperature range. From the relaxation times (τ), the activation parameters were derived using an Arrhenius fit for the β relaxation and a VFT fit for the α relaxation (see Figure 4). The fit parameters for the two high-temperature relaxations are given in Table 1.

2D Fit for γ and δ Relaxation. At temperatures below the β relaxation the peak assignment becomes more difficult. Abdul Jawad et al. did not find a γ relaxation. Our measurements however reveal the existence of a γ relaxation. Closer examination of the temperature scans at the lowest frequencies even reveals a fourth relaxation. The use of a new fit procedure made it even more clear that we are dealing with four peaks instead of the earlier reported[14] three. This is not so surprising, since the polymer is made of three monomer units.

The H−N parameters for the two low-temperature relaxations are more difficult to obtain. Fits of strongly overlapping broad and weak relaxation peaks typical for secondary relaxations are generally obscured by a limited data accuracy and a limited frequency range. By contrast, plots of ϵ'' vs temperature at sufficiently low frequencies often reveal unexpected details which imply the existence of better separable relaxation processes than visible in the frequency domain. Schlosser et al.[24] have shown that, in principle, one can always model loss spectra $\epsilon''(T)$ by using relaxation functions

(e.g. HN-functions) which contain temperature dependent parameters, e.g. $\tau(T)$, $\Delta\epsilon(T)$, or even temperature dependent shape parameters $\alpha_{HN}(T)$ and $\beta_{HN}(T)$. In a more practical approach only the relaxation time $\tau(T)$ is taken temperature dependent and is assumed to obey Arrhenius behavior for secondary relaxations. Thus combining eqs 2 and 3 leads to a temperature-dependent permittivity function. As demonstrated by Schlosser et al. this function may be used to fit several thermally activated relaxation processes, while keeping the parameters $\Delta\epsilon$, α_{HN}, and β_{HN} temperature independent.

We have incorporated this approach in a "global" fitting strategy. This so-called **2D fit** uses both the frequency **and** the temperature domain (i.e. in two dimensions) to fit the data. Temperature scans at six different frequencies are fitted simultaneously using three H−N functions (for the β, γ, and δ relaxation respectively). The best fit is found when the value of M in

$$M = \sum_{f=1}^{6} \sum_{T=1}^{40} (\epsilon_{meas}'' - \epsilon_{HN}'')^2 \qquad (10)$$

reaches a minimum.

The H−N parameters previously obtained for the β relaxation were used, as well as two Arrhenius relations for the temperature dependence of the γ and δ relaxation. This fitting procedure yielded plots of the dielectric loss vs the temperature at six different frequencies. These plots are shown in Figure 3. The fit parameters derived from this procedure (listed in Table 1) are all temperature independent. Furthermore, we have ignored the simple $1/T$ dependence of the relaxation strength, predicted by the Onsager theory. However, for secondary relaxations, this dependence is often (over)compensated by an opposite trend ($\Delta\epsilon \propto T$), caused by a decrease steric hindrance. Ignoring the influence of the temperature may result in slightly inaccurate values of $\Delta\epsilon$ for all relaxations. However, we only use these values relative to each other.

The overlapping of the three secondary relaxations may increase the uncertainties in the fitting parameters. In particular, the parameters of the γ relaxation are strongly affected by the shape and magnitude of the adjacent relaxations. However, due to the "global" fitting strategy, which ranges over 200 °C in temperature and three decades in frequency, the uncertainties are minimized. Furthermore, there is no other way to obtain the fitting parameters of the two weakest secondary relaxations more accurately. The estimated uncertainties in the fitting parameters are also given in Table 1. This shows that although the fitted peaks were strongly overlapping, the fitting results are rather accurate.

In Figure 4 the Arrhenius plots of the relaxation times vs the inverse of the temperature are shown. It appears that all four relaxations cluster at more or less the same frequency and temperature (in the temperature range from 170 to 220 °C and frequency range from 0.1 to 10 MHz). Since measurements above 1 MHz were not possible, we have no information about the behavior of the relaxations after the crossover. The most likely scenario is that all local processes merge with the main (α) relaxation and proceed as a joint single relaxation process. It is often observed that the α and β relaxation merge together, but here also two secondary relaxations collapse into one relaxation.

The steady rise in the dielectric loss at high temperatures and low frequencies (Figure 2) is caused by ionic conduction. This causes also an increase in the permittivity due to electrode polarization. The ions will accumulate at the sample−electrode interface.

Assignment of the γ and δ Relaxation. Now we will relate the γ and δ relaxation to the rotation of specific chain moieties. The rotation of the HNA moiety was already attributed to the β relaxation. The two monomer units left are the TA and the AP units. Figure 5 shows possible configurations in which the TA and AP units appear in the polymer. Hummel and Flory[25] calculated the energies for free rotation around molecular bonds in aromatic amides and esters. These energies are also depicted in Figure 5. The rotation around the $O_{ester}-C_{phenylene}$ (I) bond requires the least energy (5 kJ/mol). Rotations around the $C_{amide}-C_{phenylene}$ (II) and $N_{amide}-C_{phenylene}$ (III) bonds have identical energy barriers (11 kJ/mol). The highest rotation energy corresponds to the $C_{ester}-C_{phenylene}$ (IV) bond (22 kJ/mol). These results only account for the rotation energy and do not include any other energy contribution, such as bending or stretching. Banwell et al.[26] showed that the magnitude of these energies are comparable for most molecular bonds, so we can still use the rotation energies as an indication for the assignment of the various bond rotations. Comparing these energies for free, unhindered rotation suggest that most of the motion in the polymer takes place around the $O_{ester}-C_{phenylene}$ bonds. This leads to the following explanation of the γ and δ relaxation in the solid state: one is caused by the rotation of the TA group while the other involves the combined TA−AP group.

To find out which relaxation process corresponds to which group, we have compared our measurements with those from other authors. Several authors have performed dielectric and dynamic mechanical measurements on poly(ethylene terephthalate).[27,28,29] They all found an activation energy for the β relaxation of about 58 kJ/mol and a τ_∞ of about 10^{-16} s. Measurements on poly(butylene terephthalate)[30−32] gave an activation energy for the β relaxation of about 52 kJ/mol and also a τ_∞ of about 10^{-16} s. This indicates that the moving moiety for the β relaxation in PET and PBT is the TA group. The activation energy in PET is slightly higher than in PBT because the polymer chains are less flexible. In Vectra B950 the flexibility of the polymer chains is even less than in PET, so we can expect an even higher activation energy. This would indicate that the γ relaxation (70.8 kJ/mol) is due to the rotation of the TA group. This result is supported by data from Green.[7] He found in dielectric measurements on a copolymer made of HBA, TA and dihydroxynaphthalene a shoulder on the HBA relaxation at 0 °C and 1 Hz. This shoulder was assigned to the TA groups. Its peak position corresponds to that of the γ relaxation in Vectra B950.

Proof for the δ relaxation is less straightforward. The rotation of a combined TA−AP group is comparable with that of two HBA units in Vectra A900, as can be seen in Figure 5. The γ relaxation in Vectra A900 is probably caused by a rotation of two units, because the rotation of only one unit involves bending of the oxygen phenylene bond, which increases the rotation energy. The activation parameters for Vectra A900 can be found in the literature, e.g. Willems[33] and Kalika.[3] The activation energy of the γ relaxation is 47 kJ/mol, which is

comparable to that of the δ relaxation in Vectra B950. The preexponential factor of the Arrhenius plots is a measure for the size of the moving moiety.[34] When we compare the τ_∞ from our δ relaxation ($10^{-11.5}$ s) to a value of τ_∞ of $10^{-11.6}$ s for the γ relaxation in Vectra A900, we find a very good agreement. The preexponential factor for the γ relaxation in Vectra B950 is smaller than for the δ relaxation, indicating the rotation of a smaller group. This also points at the combined TA−AP group for the δ relaxation.

Further evidence for this molecular assignment can be found by consideration of the chain statistics. This shows that 12.8% of the TA groups are bonded by two ester groups, 6.4% have one ester and one amide bond and only 0.8% have two amide bonds. Using the dipole moments and the angles from Figure 5, we can estimate the dipole moments of the entire groups. This yields for the TA group a dipole moment of 3.6 D (2×1.8, since the angle between dipole moment and chain axis is 90°). For the combined TA−AP group, this is 5.1 D ($1.8 + 3.7 \sin(75°)$). This leads to a proposed ratio of the relaxation strengths of 1.4 ($= 3.6 \times 0.128/5.1 \times 0.064$). The ratio of the measured relaxation strengths is 1.3 (0.34/0.26). This excellent agreement supports our peak allocation. The chain moieties involved in the β, γ, and δ relaxation of Vectra B950 are summarized in Figure 6.

The value of the preexponential factor as an indication for the size of the rotating group holds only for local relaxation processes, which show typical values for τ_∞ around the IR response of 10^{-13}s. Preexponential factors of 10^{-16} or even 10^{-21} found for the β and α relaxation require another physical explanation. Schönhals et al.[35,36] have shown that side-chain liquid crystalline polymers show similar low preexponential factors, which they attribute to highly cooperative reconfiguration processes within the mesophase. The cooperative rotations of the β relaxation is the result of the amount of HNA groups. There is a high energy barrier (131 kJ/mol) for the rotation of the first group, probably caused by the existence of hydrogen bonds, but the motion of this group induces motions of similar units in its vicinity. This causes a domino effect.

TSD Experiments. The use of TSD experiments makes it possible to verify the dielectric results. Before we can attribute the peaks appearing in the TSD thermograms, we must first know the nature of these peaks (charge (ρ) or dipole).

Dipole vs Charge Relaxations. During the depolarization of a charged polymer sample, two phenomena may occur. Both the oriented dipoles as well as the frozen-in space charges can give rise to a peak in the current vs temperature plot. It is important to make a distinction between the two discharge currents.

A first series of experiments from which a distinction could be made was performed on a compression molded sample (C1). The sample was poled at 200 °C using an electric field of 1V/μm. After the sample was cooled to −100 °C, the electric field was reversed and the sample heated to 200 °C again. This yielded a first charging current. The sample was again cooled to −100 °C, after which the electric field was switched off. Next, a second, discharging current was recorded by reheating to 200 °C again. The measured currents are shown in Figure 7. As can be seen, the first current after reversal of the field (curve a) is twice as high as the second current (curve b) for temperatures ranging from −100 °C to the peak at +144 °C. This is an indication that in this range the current is caused by dipole reorientation. The dipoles are oriented in the direction of the applied field. When the field is switched off, the dipoles tend to reorient themselves randomly. However, upon reversal of the electric field, the dipoles will realign in the reversed electric field and produce a current twice as high. This doubling of the current will not appear entirely for a charge relaxation, since charges can recombine when the field is reversed.

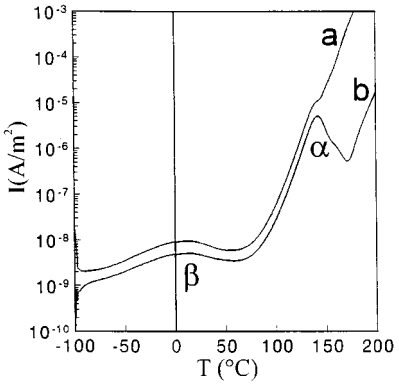

Figure 7. Current density vs temperature for sample C1. The sample is first poled at 200 °C and +1 V/μm and then cooled to −100 °C with the electric field on. The field is then reversed to −1 V/μm and the sample heated to 200 °C while measuring the charging current (curve a). The sample is then cooled to −100 °C after which the electric field is switched off. Finally the sample is reheated to 200 °C to measure the discharge current (curve b). The signs of the curves were actually opposite.

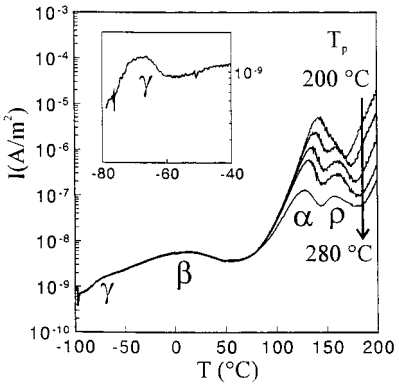

Figure 8. Depolarization current density vs temperature of one C1 sample for five different poling temperatures: 200, 220, 240, 260, and 280 °C. The insert shows an enlargement of the γ relaxation.

The TSD peak at 15 °C can be attributed to the β relaxation, whereas the peak at 144 °C corresponds to the α-relaxation. The two other relaxations are shifted to such low temperatures that they do not show up in the temperature range chosen.

Also, from another series of measurements on a C1 sample, proof for both dipole and charge relaxations was found. This was done by five consecutive experiments on one sample, while varying the polarization temperature (T_p). This temperature can have a marked influence on the depolarization current. This can be seen in Figure 8. Five curves are depicted for polarization temperatures, ranging from 200 to 280 °C. The first point that appears from the figure is that the position and magnitude of the β relaxation does not depend on the polarization temperature. Also, the onset

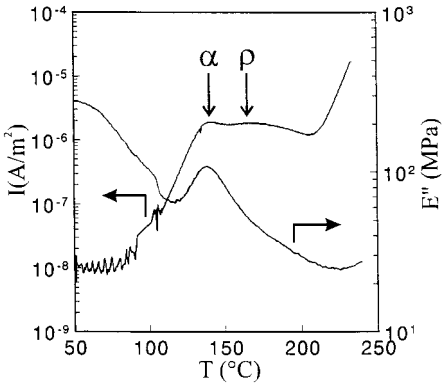

Figure 9. Simultaneous TSD (current density) and DMA (loss modulus) experiment on a compression molded sample (C1) poled at 240 °C.

of the α peak is independent of the polarization temperature. This is another indication that dipole reorientation is involved.

Combined TSD and DMA Experiments. The second striking observation from Figure 8 is the splitting up of the high temperature peak into two peaks for the higher polarization temperatures. Before discussing this phenomenon in detail, we should first discuss the nature of the two peaks involved. We have to distinguish between dipole and charge relaxations. Since the onset (between 50 and 100 °C) of the lower temperature peaks remains practically the same, this is most probably a dipole peak.

The high temperature peak is less clear. To elucidate the nature of this peak, we have performed TSD and DMA experiments simultaneously. We have poled a compression-molded sample (C1) at 240 °C inside the DMA setup. The depolarization current and the dynamic mechanical loss modulus during heating of the sample are presented in Figure 9. In the first part of the graph, the current shows a lot of noise. This is caused by a combination of a low value of the signal itself and the measuring setup used. Between 125 and 200 °C, two peaks are visible in the depolarization current (arrows in Figure 9), whereas in the same temperature range only one peak is visible in the mechanical loss modulus. This peak can be attributed to the glass transition or α-relaxation. The second peak from the TSD experiment is absent in the DMA curve. This is an indication that this peak is due to charge motions. The movement of charges cannot be seen in mechanical measurements, because it has no influence on the motion of the polymer chains. So, we can conclude that at high poling temperatures, a low-temperature dipole peak and a high-temperature charge or ρ peak appear in the TSD thermogram.

Another support for the just mentioned TSD peak assignment comes from a spontaneous depolarization experiment (see e.g. Kim[37] and Van Turnhout[21,pp199−200]). A compression-molded sample (C1) is heated to 260 °C without an electric field, during which the depolarization current is recorded. This thermogram showed that the two peaks between 100 and 175 °C had opposite signs. This again means that one peak (the first) is a dipole and the other (the second) is a charge relaxation peak.

TSD vs Dielectric Experiments. As already stated in the theoretical section, the TSD experiments are comparable to dielectric measurements at a very low frequency. We will now deal with the various relaxations separately.

Table 2. Polarization Temperatures of the TSD Experiments, Measured and Calculated Temperatures at Current Maximum, and Depolarization Currents

		T_m (°C)			I_m (nA/m²)	
peak	T_p (°C)	(meas)	(calc)[a]	ω_m[b] (rad/s)	(meas)	(calc)[c]
α	200	144	125	0.0175	5250	23
	220	138	125	0.0175	2480	23
	240	135	125	0.0175	1210	23
	260	132	125	0.0175	590	23
	280	128	125	0.0175	96	23
β		15	17	0.0062	5.8	5.9
γ		−70	−57	0.0061	1.6	1.3
δ			−134	0.0084		0.8

[a] The temperature at the current maximum is calculated using the value of $\omega_m\tau$ from Table 1 and eqs 4 and 7 for the α relaxation and eqs 3 and 6 for the secondary relaxations. Note that T_m = 128 °C of the α peak agrees well with T_g = 131 °C from DSC. [b] The angular frequency at current maximum is calculated using eq 6 or 7. [c] The depolarization current is calculated using eq 9 and ϵ''_{max} from Table 1.

α Relaxation. The frequency of the dielectric measurements at which the loss peak will be at the same position as the current peak in the TSD measurements, can be calculated using eq 7. Figure 8 shows that the shift of the position of the dipole peak depends on the polarization temperature. Therefore, we must consider each peak separately. The values for the different parameters can be obtained from Table 1: E_V = 46.9 kJ/mol, T_V = 294 K, and h = 30 s/K. Using eq 8, we can calculate for the peak maximum for the α relaxation: $\omega_m\tau = 9.2$. Using this value and eqs 4 and 7, we can obtain the theoretical value of the temperature at peak maximum. Subsequently, the value for the angular frequency at the current maximum can be calculated using eq 7. This peak temperature and frequency at current maximum are listed in Table 2. Finally from eq 9 we obtained the height of the current maximum, using the value of $\epsilon_m'' = 0.220$ found from the HN relation. All of the previously calculated and measured parameters are listed in Table 2.

Close examination of Figure 8 and Table 2 leads to a few observations. First, the current maximum shifts toward lower temperatures with increasing polarization temperature. Furthermore, the current maxima themselves decrease with increasing T_p. When the measured T_m and I_m are compared with the calculated values (Table 2), it becomes clear that both agree best with the peak at the highest polarization temperature. The deviation from the theory (eq 9) is the highest at the lowest T_p. This leads to the conclusion that the correct position and magnitude of the dipole depolarization peak is best measured using a high polarization temperature, possibly even higher than 280 °C. A decrease of this temperature results in a shift of the position and magnitude of the peak. This is a very important conclusion for further discussion of the TSD experiments. We can also conclude that the magnitude and position of the α relaxation is strongly determined by the existence of free charges in the polymer. The α peak increases when the charge or ρ peak increases. In a forthcoming publication we shall pay more attention to these charge effects. In this paper we will only deal with dipole relaxations.

***β* and *γ* Relaxation.** The same evaluation of the TSD data as in the previous section has been performed for the secondary relaxations. Figure 8 locates the β

peak at 15 °C. It seems that a second peak is visible at approximately −70 °C. After zooming in on this temperature range this peak becomes more clear (see inset in Figure 8). However, the maximum temperature and current are not very accurate, because this peak emerges as a shoulder on the β peak. For the evaluation of the β peak data, we used eqs 3, 6, and 8, $\omega_m\tau = 2.4$, and $\epsilon_m'' = 0.159$. The values of the measured temperature and magnitude of the current maximum compare very well with the calculated ones. For the γ relaxation we calculated with eq 8 from the HN relation: $\omega_m\tau = 17$ and $\epsilon_m'' = 0.035$. It is surprising that, although the activation energies and peak temperatures of the β and γ relaxation are different, the angular frequencies at the current maxima are the same for both relaxations ($\omega_m \approx 0.006$). For the δ relaxation, the calculated temperature at which the current in the TSD experiments should show a maximum is −134 °C. This temperature lies beyond our TSD scan. Furthermore, the calculated current for the δ relaxation would be approximately 0.8 nA/m^2, which is rather low to be measured accurately. The difference between the calculated and the measured current maximum of the γ peak is caused by superposition of this peak with the onset of the β peak.

When we compare the dielectric (Figure 2) and the TSD (Figure 7) results of the α and β relaxations, it is clear that the relaxation peaks are completely separated in the TSD experiments. This is caused by the big difference in the activation energies of the two relaxations. This separation is less visible for the low-frequency dielectric results (Figure 2), because ionic conduction obscures the α relaxation.

V. Conclusions

The thermotropic liquid crystalline copolyesteramide Vectra B950 was studied with dielectric and TSD measurements. The use of a broad frequency range and a new fit strategy made it possible to obtain information about two additional secondary relaxations besides the already known α and β relaxations. The fit procedure involves simultaneous fitting of a number of temperature scans at different frequencies. The use of dipole moments, rotational energies, and statistics, together with information about relaxations from the literature, made it possible to attribute the low-temperature relaxations to rotations of the terephthalic acid and aminophenol groups.

The TSD experiments confirmed the dielectric observations concerning the secondary relaxations. However, the TSD experiments around the glass transition temperature are not simply comparable to the dielectric results, possibly due to interference of the dipole and charge relaxations. The polarization temperature has a significant influence on the position and magnitude of the α peak.

Acknowledgment. This work was sponsored by The Netherlands Organization of Scientific Research (SON/STW-NWO).

References and Notes

(1) Blundell, D. J.; Buckingham, K. A. *Polymer* **1985**, *26*, 1623−1627.
(2) Alhaj-Mohammed, M. H.; Davies, G. R.; Abdul Jawad, S.; Ward I. M. *J. Polym. Sci., Polym. Phys. Ed.* **1988**, *26*, 1751−1760.
(3) Kalika, D. S.; Yoon, D. Y. *Macromolecules* **1991**, *24*, 3404−3412.
(4) Troughton, M. J.; Davies, G. R.; Ward, I. M. *Polymer* **1989**, *30*, 58−62.
(5) Wissbrun, K. F.; Yoon, H. N. *Polymer* **1989**, *30*, 2193-2197.
(6) Sarlin, J.; Törmälä, P. J. *Mater. Sci. Lett.* **1992**, *11*, 671−673.
(7) Green, D. I.; Davies, G. R.; Ward, I. M.; Alhaj-Mohammed, M. H.; Abdul Jawad, S. *Polym. Adv. Technol.* **1990**, *1*, 41−47.
(8) Takase, Y.; Mitchell, G. R.; Odajima, A. *Polym. Commun.* **1986**, *27*, 76−78.
(9) Bechtoldt, H.; Wendorff, J. H.; Zimmermann, H. J. *Makromol. Chem.* **1987**, *188*, 651−663.
(10) Kalika, D. S.; Shen, M.-R.; Yu, X.-M.; Denn, M. M.; Iannelli, P.; Masciocchi, N.; Yoon, D. Y.; Parrish, W.; Friedrich, C.; Noël, C. *Macromolecules* **1990**, *23*, 5192−5200.
(11) Kalika, D. S.; Yoon, D. Y.; Iannelli, P.; Parrish, W. *Macromolecules* **1991**, *24*, 3413−3422.
(12) Gonzalez, J. M.; Muñoz, M. E.; Cortazar, M.; Santamaría, A.; Peña, J. J. *J. Polym. Sci., Polym. Phys. Ed.* **1990**, *28*, 1533−1550.
(13) Abdul Jawad, S. *Polym. Int.* **1994**, *33*, 373−376.
(14) Abdul Jawad, S.; Alhaj-Mohammed, M. H. *Mater. Lett.* **1992**, *13*, 312−317.
(15) Sauer, B. B.; Dipaolo, N. V.; Avakian, P.; Kampert, W. G.; Starkweather, H. W., Jr. *J. Polym. Sci., Polym. Phys. Ed.* **1993**, *31*, 1851−1859.
(16) Sauer, B. B.; Beckerbauer, R.; Wang, L. *J. Polym. Sci., Polym. Phys. Ed.* **1993**, *31*, 1861−1872.
(17) Collins, G.; Long, B. *J. Appl. Polym. Sci.* **1994**, *53*, 587−608.
(18) Ibar, J. P. *Fundamentals of Thermal Stimulated Current and Relaxation Map Analysis*; SLP Press: New Canaan, CT, 1993; pp 169−179.
(19) Shimizu, H.; Kitano, T.; Nakayama, K. *Jpn. J. Appl. Phys.* **1996**, *35* (2), L231-L233.
(20) Moura Ramos, J. J.; Mano, J. F.; Sauer, B. B. *Polymer* **1997**, *38* (5), 1081−1089.
(21) van Turnhout, J. *Thermally Stimulated Discharge of Polymer Electrets*; Elsevier: Amsterdam, 1975.
(22) van Turnhout, J. In *Electrets, Topics in Applied Physics*; Sessler, G. M., Ed.; Springer: Berlin, 1987; Vol. 33, pp 106−135.
(23) Havriliak, S., Jr.; Havriliak, S. J. *Dielectric and Mechanical Relaxations in Materials*; Hanser Publishers: Munich, 1997; Germany, pp 54−57.
(24) Schlosser, E.; Schönhals, A.; Carius, H. E.; Goering, H. *Macromolecules* **1993**, *26*, 6027−6032.
(25) Hummel, J. P.; Flory, P. J. *Macromolecules* **1980**, *13*, 479−484.
(26) Banwell, C. N. *Fundamentals of Molecular Spectroscopy*, 3rd ed.; McGraw-Hill: London, 1983; p 109.
(27) Tatsumi, T.; Ito, E.; Hayakawa, R. *J. Polym. Sci., Polym Phys. Ed.* **1992**, *30*, 701−706.
(28) Carius, H. E.; Schönhals, A.; Guigner, D.; Sterzynski, T.; Brostow, W. *Macromolecules* **1996**, *29*, 5017−5025.
(29) Ezquerra, T. A.; Baltà-Calleja, F. J.; Zachmann, H. G. *Acta Polym.* **1993**, *44*, 18−24.
(30) Ezquerra, T. A.; Roslaniec, Z.; López-Cabarcos, E.; Baltà-Calleja, F. J. *Macromolecules* **1995**, *28*, 4516−4524.
(31) Gallagher, K. P.; Zhang, X.; Runt, J. P.; Huynh-ba, G.; Lin, J. S. *Macromolecules* **1993**, *26*, 588−596.
(32) Pratt, G. J.; Smith, M. J. A. *Polymer* **1989**, *30*, 1113−1116.
(33) Willems, C. R. J. A Dielectric Study of Melting and Crystallization of Semirigid and Flexible-Chain Polymers. Ph.D. Thesis, Delft, The Netherlands, 1995.
(34) Böttcher, C. J. F.; Bordewijk, P. *Theory of Electric Polarization*, 2nd ed.; Elsevier: Amsterdam, 1978; Vol. II, p 225.
(35) Schönhals, A.; Gessner, U.; Rübner, J. *Macromol. Chem. Phys.* **1995**, *196*, 1671−1685.
(36) Schönhals, A.; Wolff, D.; Springer, J. *Macromolecules* **1995**, *28*, 6254−6257.
(37) Kim, E. J.; Takeda, T.; Ohki, Y. *IEEE Trans. Dielectr. Electron. Insul.* **1996**, *3* (3), 386−391.

MA9716138